Numerical Study on Laser-driven In-Tube Accelerator (LITA) Performance using a Plasma Size Modeling

Sukyum Kim, Toshiro Ohtani**, Akihiro Sasoh**, In-Seuck Jeung* and Jeong-Yeol Choi****
**Department of Aerospace Engineering, Seoul National University, Seoul, Korea*
***Ultra-High-Enthalpy Flow Laboratory, Institute of Fluid Science, Tohoku University, Sendai, Japan*
****Department of Aerospace Engineering, Pusan National University, Busan, Korea*
Department of Aerospace Engineering, Seoul National University, Seoul 151-744, Korea
newstd999@hotmail.com

Keywords: Laser Propulsion, Plasma, LITA

Abstract

Laser Propulsion is a device that generates thrust using laser energy. Laser-driven In-Tube Accelerator (LITA) has been developed at Tohoku University. LITA is a laser propulsion system that accelerates an object not in an open air but in a tube. Experiments of vertical launching and pressure measurement on the tube wall were carried out and in order to observe the initial state of plasma and blast wave, the visualization experiment was carried out using the shadowgraph method. In this study, the time variation of pressure on the tube wall is numerically simulated solving Euler equation. In order to model the laser energy, heat source function added to the frozen flow Euler equation. Plasma size from the shadowgraph images was used for the initial condition of laser energy input. For verification of the modeling, these results were compared with the previous experimental and numerical results. From these verifications, an analysis of LITA performance will be investigated.

Introduction

Laser Propulsion is a device that generates thrust using laser energy. Kantrowitz[1)] proposed this idea in 1972. One of the main studies on laser propulsion system is to generate propulsive power from laser induced plasma. The first flight test was carried out by Myrabo et al. in 1998[2-3)]. After that, various launch experiments have been carried out[4-6)].

Laser-driven In-Tube Accelerator (LITA) has been developed at Tohoku University. LITA is a laser propulsion system that accelerates an object not in an open air but in a tube[7-11)]. LITA have several characteristics such that the driver gas can be changed and the operation pressure can be selected. When the laser beam focused on a focal point, the driver gas becomes plasma state. Free electrons enhance laser energy absorption and breakdown occurs. A blast wave is induced by the plasma expansion. Thrust is generated since the blast wave makes pressure difference between frontal and rear side of projectile.

In this paper, the time variation of pressure on the tube wall is numerically simulated solving Euler equation. Plasma size from the shadowgraph images was used for the initial condition of laser energy input[12-13)]. And this modeling is compared with experimental results and previous modeling.

Experimental Setup

Vertical launch experiments, overpressure measurements and shadowgraph experiment have been carried out. A CO2 TEA laser was used in these experiments. This laser generates 5J/pulse energy and 100Hz repetition frequency.

Fig. 1 shows the schematic of the experimental setup. The laser beam is vertically introduced to the tube by molybdenum mirrors. The material of the acceleration tube is acryl. It has an inner diameter of 25.2mm to 25.4mm and a length of either 0.5m or 1.0m. A tube end which the laser beam is introduced is plugged with a NaCl window, the other end with a brass flange. The pressure measurement device is attached to the acceleration tube below the projectile position. The detailed arrangement in the pressure measurement assembly is shown in Fig. 2. The projectile is initially placed above the pressure transducer. The pressure transducer is mounted in an aluminum tube. In the experiment, a piezoelectric pressure transducer (PCB) was used. The PCBs were mounted on the wall 14.7mm below the focal point of projectile. An *overpressure history* is measured in a single shot only in the rear incident operation.

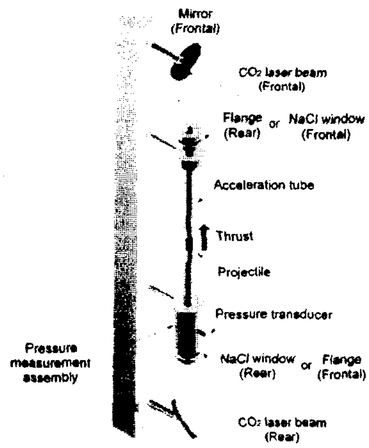

Fig. 1 The schematic of experimental setup

Fig. 3 shows the schematics of shadowgraph experiment. Visualization was carried out using high speed camera. The laser beam is introduced form upper side that is plugged with the NaCl window. This experiment performed on two types of projectile model but in this study used only rear incidence type.

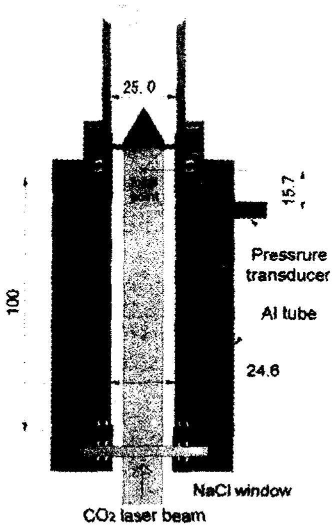

Fig. 2 The detailed view of pressure measurement device

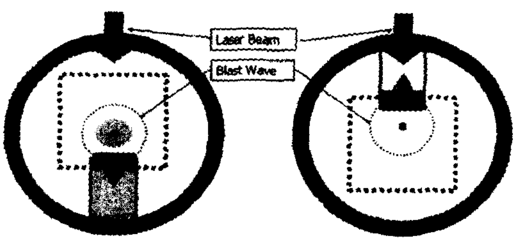

Fig. 3 Experimental setup for shadowgraph experiment

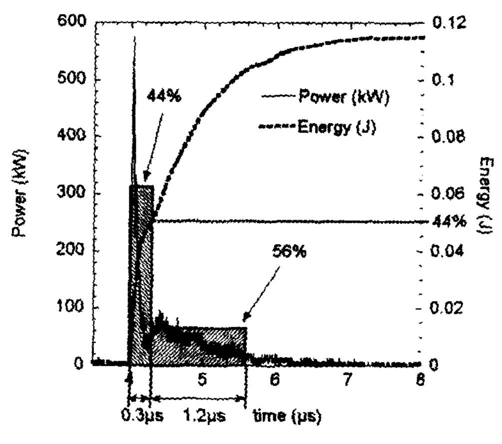

Fig. 4 Time variation of laser power and numerical modeling

Fig. 4 shows the measured laser power and accumulated laser energy with photon drag sensor. (Hamamatsu B749). Total laser energy input is measured also with the energy meter (Gentic ED-500LIR) and the laser energy is 5J. Fig. 3 shows small accumulated laser energy because the sensing area of photon drag sensor is about 1/30 of the laser beam size. Therefore, this energy is only part of total laser energy. From the Fig. 3, about 44% energy input is concentrated in the first peak with 0.3μs time range and another 56% of energy input continues 2 or 3μs. So, time variation of power can be simplified as a shaded rectangular shape like Fig. 3 for the numerical study.

Numerical Modeling

In this study the small viscous effect can be assumed because the impulse generation is governed mainly by the shock shock wave structure. Therefore, Euler equation for an axi-symertric geometry is used for governing equation. In order to model the laser energy, heat source function added to the frozen flow Euler equation.

$$\frac{\partial \mathbf{Q}}{\partial t}+\frac{\partial \mathbf{F}}{\partial x}+\frac{\partial \mathbf{G}}{\partial y}+\alpha \mathbf{H}=\mathbf{W}$$

$$\mathbf{Q}=[\rho,\ \rho u,\ \rho v,\ e\ ]^T, \mathbf{W}=[0,\ 0,\ 0,\ q\ ]^T$$

$$\mathbf{F}=[\rho u,\quad \rho u^2+p,\quad \rho uv,\quad (e+p)u]^T$$

$$\mathbf{G}=[\rho v,\quad \rho uv,\quad \rho v^2+p,\quad (e+p)v]^T$$

$$\mathbf{H}=[\rho v,\quad \rho uv,\quad \rho v^2,\quad (e+p)v]^T$$

The heat source function is modeled from the measured data using photon drag sensor (Hamamatsu B749). This modeling is explained above.

The governing equations are discretized by finite volume method and the numerical fluxes are calculated by Roe's scheme at computational cell interfaces. For the higher order spatial accuracy while maintaining TVD characteristics, MUSCL (monotone upstream centered schemes for conservation laws) interpolation scheme is used with minmod limiter function[14]. Time marching was carried out by the Crank-Nicolson method, a simplest form of the second-order-accurate, implicit time integration method.

Model of Plasma Size

Fig. 5 shows shadowgraph images of laser induced plasma. The framing interval is 50ns and total time is 400ns. From this image, we can confirm the initial plasma creation is very fast. It takes only 50ns or 100ns and after that their size are almost uniform. From the laser energy measurement, time range of laser input is about 3μs and laser energy absorption occurs mainly in the plasma region since free electron enhance the laser beam absorption. Fig. 6 shows the shadowgraph images of laser induced blast wave. The initial blast wave shows similar shape with initial plasma.

Numerical modeling of initial plasma using these assumptions is shown in Fig. 7. In the previous simulation[10], simple sphere model of 3mm diameter was used. In this study, from the shadow graph image, cone type heat source model of 5mm diameter was used.

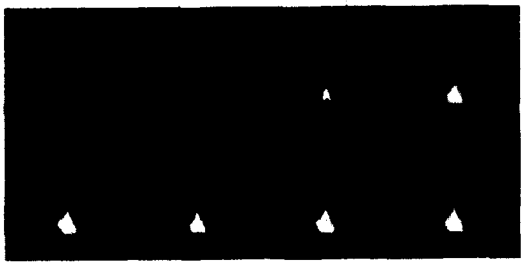

Fig. 5 Shadowgraph images of laser induced plasma and blast wave (Driver gas : Xenon, Fill pressure : 100kPa, Framing interval : 50ns, Laser energy : 3J)

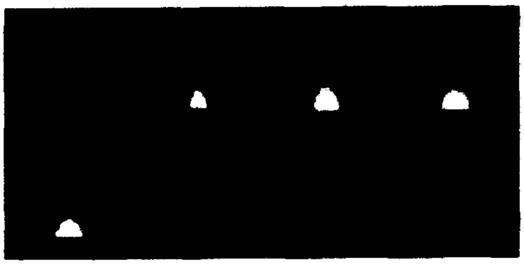

Fig. 6 Shadowgraph images of laser induced plasma and blast wave (Driver gas : Xenon, Fill pressure : 100kPa, Framing interval : 1μs, Laser energy : 3J)

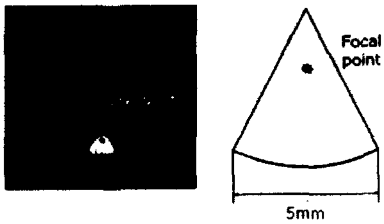

Fig. 7 Plasma size modeling from the shadowgraph image

The corresponding computational domain is shown in Fig. 8. In this calculation, two zones are used. 111×71 and 250×250 grids are used for zone 1 and 2. The inflow boundary condition is fixed, solid walls (projectile, tube) is slip line condition and outflow zeroth-order extrapolation. Two types of plasma size model were calculated. First model has heat source area of sphere shape and second model has cone shape heat source

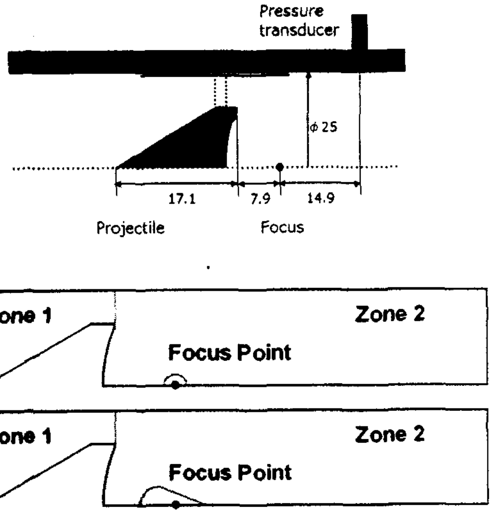

Fig. 8 Projectile geometry and computational domain and two different modeling of plasma size

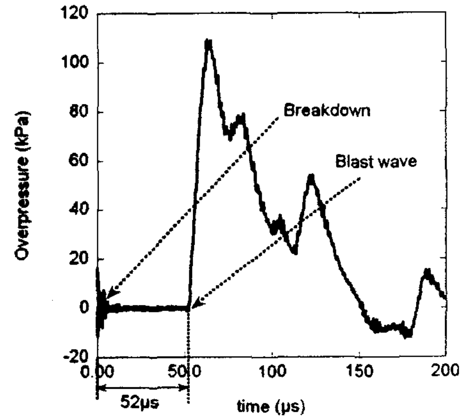

Fig. 9 Time range from breakdown to the first peak (Driver gas : Xenon, Fill pressure : 100kPa)

The time range from breakdown to first peak is shown in Fig. 9. This time duration is determined by initial shock wave strength. The effective laser energy that used to create blast wave is only small fraction. The effective laser energy could be found by the comparison of the time from breakdown to pressure peak of the over pressure history between numerical and experimental results.

Result

In this calculation, Xenon gas was used for driver gas and fill pressure was 100kPa. 50% fraction of laser energy is assumed for efficient input[13]. Fig. 10 shows the overpressure history. This shows good time agreement of first peak time and next following peak times of reflected shock waves. This means the shock wave strength of experiment and numerical simulation is almost same. So, we can guess determined effective input is reasonable.

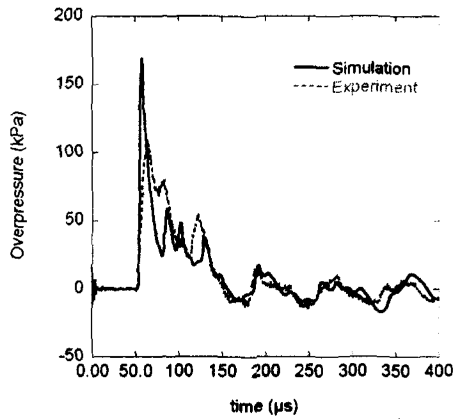

Fig. 10 Overpressure history of experiment and numerical simulation in the case of cone model of plasma (Driver gas : Xenon, Fill pressure : 100kPa, 50% of laser energy).

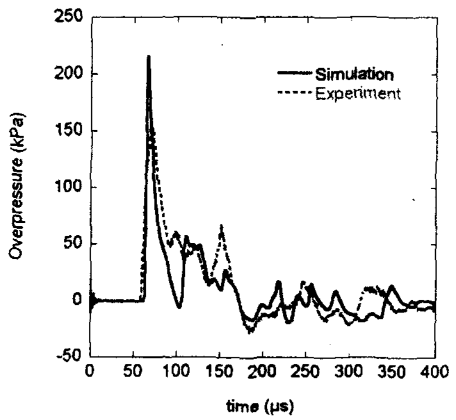

Fig. 111 Overpressure history of experiment and numerical simulation in the case of cone model of plasma (Driver gas : Xenon, Fill pressure : 200kPa, 50% of laser energy).

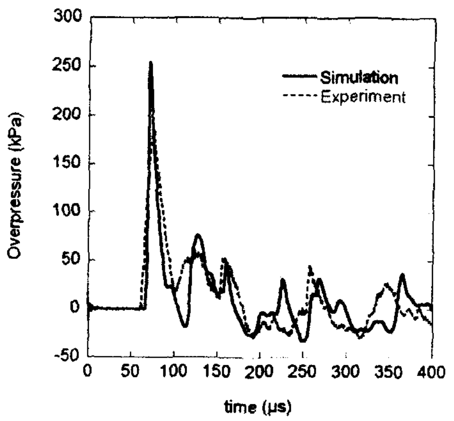

Fig. 122 Overpressure history of experiment and numerical simulation in the case of cone model of plasma (Driver gas : Xenon, Fill pressure : 300kPa, 50% of laser energy).

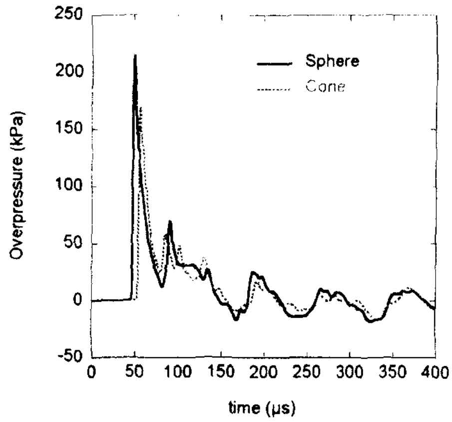

Fig. 133 Overpressure history of sphere and cone model using the same effective laser energy input (Driver gas : Xenon, Fill pressure : 100kPa , 50% of laser energy)

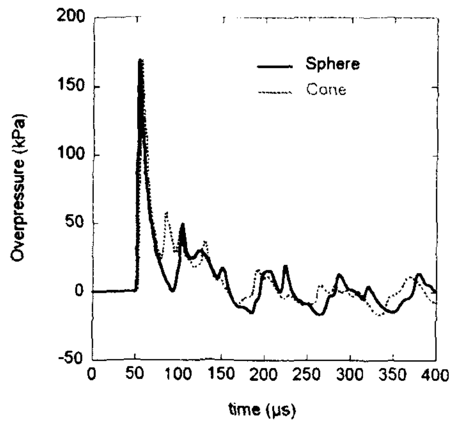

Fig. 144 Overpressure history of sphere and cone model in the case that have the same peak value (Driver gas : Xenon, Fill pressure : 100kPa , Cone : 50% of laser energy, Sphere : 30% of laser energy)

Fig. 11 and Fig. 12 show the different fill pressure cases. And these results show small difference about time between numerical and experimental case. So, improvement of modeling will be needed.

Fig. 13 shows the comparison of overpressure history of sphere and cone model of heat source using the same effective laser energy input (50% fraction of laser energy, 1.2J). This shows the faster shock wave speed until the first peak in the case of the sphere heat source but reflected shock wave becomes slow and time is almost same between these two cases. In Fig. 14, it is shown that two cases have the same peak value. In the sphere case, assumed effective laser input is 30% of the laser energy[10]. This graph shows that two cases show the same peak value and almost same first peak time but the reflected shock speed is different each other. And the conical modeling shows better agreement with experimental results.

Conclusion

In this study, 1) Laser energy input modeling was enhanced and plasma area modeled from shadowgraph image. 2) Plasma size modeling is tested and compared with experimental results and previous modeling and different initial pressure case. 3) Time agreement was improved compared with the previous sphere model of heat source. 4) Numerical studies were performed about various cases. From these results, we can guess determined effective input is reasonable. But, in large initial pressure cases, this modeling shows some problems, so, remodeling of plasma area will be performed to improve the prediction of the shock wave structure.

Acknowledgement

This study was partly supported by BK21 Program sponsored by Seoul National University.

References

1) Kantrowitz, A. : Propulsion to Orbit by Ground-Based Lasers, *Astronautics and Aeronautics*: Vol.10, 1972, pp.74-76.
2) Myrabo, L. N., Messitt, D. G., and Mead, F. B. Jr., : Ground and Flight Tests of a Laser Propelled Vehicle, *AIAA paper*: 98-1001, 1998.
3) Mead, F. B. Jr., Myrabo, L. N., and Messitt, D. G., : Flight and Ground Tests of a Laser-Boosted Vehicle, *AIAA paper*: 98-3735, 1998.
4) Schall, W. O., Bohn, W. L., Eckel, H.-A. Mayerhofer, W., Riede, W., and Zeyfang, E. : Lightcraft Experiments in Germany, *High-Power Laser Ablation III, Proc. SPIE*: Vol.4065, 2000, pp.472-481.
5) Schall, W. O., Eckel, H.-A. Mayerhofer, W., and Zeyfang, E. : Pulsed Power for Space Propulsion, *International Conference on Pulsed Power Applications*: No.H.05, 2001.
6) Myrabo, L. N., Libeau, M. A., Meloney, E. D., and Bracken, R. L. : Survivability of Thin Metal Mirror Coatings on Graphite Pulsed Laser Propulsion Engines, *AIAA paper*: 2002-3783, 2002
7) Sasoh, A. : Laser-Propelled Ram Accelerator, *Journal de Physique IV*: Vol. 10, Pr11, 2000, pp.41-47.
8) Sasoh, A. : Laser-Driven in Tube Accelerator, *Review of Scientific Instruments*: Vol. 72, No.3, 2001, pp.1893-1898.
9) Sasoh, A., Urabe, N., and Kim, S. : Laser-Driven In-Tube Accelerator Operation Using Monoatomic Gases, *AIAA paper*: 2002-2201, 2002.
10) Sasoh, A., Choi, J.-Y., Jeung, I.-S., Urabe, N., Kleine, H. and Takayama, K. : Impulse Enhancement of Laser Propulsion in Tube, *Postepy Astronautyki*: Vol. 27, No. 1, 2001, pp.40-50.
11) Sasoh, A., Urabe, N., Kim, S., and Jeung, I.-S. : Impulse Scaling in Laser-Driven In-Tube Accelerator, *Applied Physics* A: Vol. 77, 2003, pp.349-352.
12) Wang, T.-S., Chen, Y.-S., Liu, J., Myrabo, L. N., and Mead, F. B. Jr. : Advanced Performance Modeling of Experimental Laser Lightcraft, *Journal of Propulsion and Power*: Vol. 18, No. 6, 2002, pp.1129-1138.
13) Katsurayama, H., Komurasaki, K., and Arakawa, Y. : Numerical Analyses on Pressure Wave Propagation in Repetitive Pulse Laser Propulsion, *AIAA paper*: 2001-3665, 2000
14) Choi, J.-Y., Jeung, I.-S., and Yoon, Y. : Computational Fluid Dynamics Algorithms for Unsteady Shock-Induced Combustion, Part I ; Validation, *AIAA Journal*: Vol, 38, No.7, 2000, pp.1179-1187.